and by the National Science Foundation (Grant CHE77-14594) for work done at Rice University and the National Science Foundation (Grant CHE77-01372) for work done at the University of Virginia.

Registry No. $[Fe^{III}(3\text{-}OCH_3Salmeen)_2]PF_6$, 65293-76-7; $[Fe^{III}(5\text{-}NO_2Salmeen)_2]PF_6$, 65293-68-7; $[Fe^{III}(5\text{-}OCH_3Salmeen)_2]PF_6$, 65293-72-3.

Supplementary Material Available: Tables of hydrogen atomic parameters, bond distances and angles within the PF_6^- anions, and observed and calculated structure factor amplitudes (37 pages). Ordering information is given on any current masthead page.

Contribution from the Department of Chemistry, University of Massachusetts, Amherst, Massachusetts 01003, and the Institut für Anorganische Chemie, Universität München, D-8000 München 2, Germany

Bridgehead Phosphorane Structures in Tetrafluoro- and Tetrachlorodiazadiphosphetidines with Fused Five-Membered Rings[1,2]

ROBERTA O. DAY,[3a] ROBERT R. HOLMES,*[3a] HELMUT TAUTZ,[3b] J. HELMUT WEINMAIER,[3b] and ALFRED SCHMIDPETER*[3b]

Received July 29, 1980

P,P-Difluoro- and *P,P*-dichloro-1,3,4,2-oxadiazaphospholes and -1,2,4,3-triazaphospholes form tricyclic dimers with two phosphorane bridgeheads joined together by a diazadiphosphetidine ring. NMR data are consistent with either meridional or facial ring placement in these pentacoordinate phosphorus derivatives. Single-crystal X-ray analysis of two members, the dimeric triazaphospholes $(PhCN_3MePF_2)_2$ (**4a**) and $(PhCN_3MePCl_2)_2$ (**4b**), reveal cis-facial structures. The pentacoordinated geometry around each phosphorus center is almost exactly halfway between the idealized trigonal bipyramid and square pyramid along the Berry coordinate. **4a** crystallizes in the monoclinic space group $P2_1/n$, with a = 11.344 (7) Å, b = 11.617 (5) Å, c = 14.254 (11) Å, β = 96.83 (6)°, and Z = 4. **4b** crystallizes in the monoclinic space group $P2_1/c$ with a = 6.585 (2) Å, b = 21.383 (9) Å, c = 15.824 (7) Å, β = 103.89 (4)°, and Z = 4. Data for both compounds were collected, with an automated Enraf-Nonius CAD 4 diffractometer, out to a maximum $2\theta_{Mo\,K\alpha}$ of 50°. Full-matrix least-squares refinement techniques led to the final agreement factors of R = 0.042 and R_w = 0.051 for **4a** on the basis of 2059 reflections having $I \geq 2\sigma_I$ and R = 0.036 and R_w = 0.046 for **4b** for the 2855 reflections having $I \geq 2\sigma_I$. The cis-facial conformation for **4a** and **4b** in contrast to the meridional form found for two related tricyclic diphosphoranes is attributed to the dominance of halogen apicophilicity over the preference for nitrogen planarity. The extent of displacement toward the square pyramid is viewed as a measure of the relative importance of these two effects. A low-energy path for intramolecular ligand exchange is suggested to account for the suspected fluxional behavior indicated by the NMR data.

Introduction

Two trigonal bipyramids having a central phosphorus atom and sharing an edge between an apical and an equatorial nitrogen atom constitute the (idealized) structure of diaza-di-λ^5-phosphetidines, Ia. These dimeric phosphoranes exist when substituents of sufficient electronegativity are attached to phosphorus. For example, X-ray and in some cases electron diffraction analyses have shown the existence of this structural class for fluoro-[4-8] and chloro-substituted[9-11] derivatives. Inclusion of a second small ring, leading to the spirocyclic structure Ib, also helps to stabilize the diazadiphosphetidine ring. X-ray analysis of several members have been reported.[12-14]

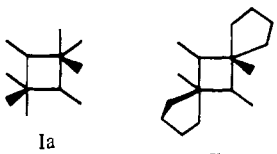

Ia Ib

An interesting and relatively unexplored conformational problem arises if two five-membered rings are fused to the diazadiphosphetidine ring, making phosphorus (and nitrogen) bridgehead atoms. These tricyclic systems can be looked upon as dimers of five-membered cyclic phosphazenes:

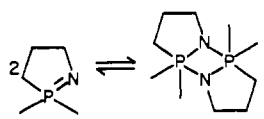

(1) (a) Pentacoordinated Molecules. 38. (b) Previous paper in this series: Day, R. O.; Husebye, S.; Holmes, R. R. *Inorg. Chem.* **1980**, *19*, 3616.
(2) (a) Four- and Five-Membered Phosphorus Heterocycles. 47. (b) Part 46: Schmidpeter, A.; Zeiss, W.; Schomburg, D.; Sheldrick, W. S. *Angew. Chem.* **1980**, *92*, 860; *Angew. Chem., Int. Ed. Engl.* **1980**, *19*, 825.
(3) (a) University of Massachusetts. (b) Universität München.
(4) Cox, J. W.; Corey, E. R. *Chem. Commun.* **1967**, 123.
(5) Almenningen, A.; Andersen, B.; Astrup, E. E. *Acta Chem. Scand.* **1969**, *23*, 2179.
(6) Sheldrick, W. S.; Hewson, M. J. C. *Acta Crystallogr., Sect. B* **1975**, *B31*, 1209.
(7) Fild, M.; Sheldrick, W. S.; Standiewicz, T. *Z. Anorg. Allg. Chem.* **1975**, *415*, 43.
(8) Harris, R. K.; Wazeer, M. I. M.; Schlak, O.; Schmutzler, R.; Sheldrick, W. S. *J. Chem. Soc., Dalton Trans.* **1977**, 517.
(9) Hess, H.; Forst, D. *Z. Anorg. Allg. Chem.* **1966**, *342*, 240.
(10) Hoard, L. G.; Jacobson, R. A. *J. Chem. Soc. A* **1966**, 1203.
(11) Weiss, J.; Hartmann, G. *Z. Anorg. Allg. Chem.* **1967**, *351*, 152.
(12) Gibson, J. A.; Röschenthaler, G.-V.; Schomburg, D.; Sheldrick, W. S. *Chem. Ber.* **1977**, *110*, 1887.
(13) Gilyarov, V. A.; Tikhonina, N. A.; Andrianov, V. G.; Struchkov, Yu. T.; Kabachnik, M. I. *J. Gen. Chem. USSR (Engl. Transl.)* **1978**, *48*, 670; *Zh. Obshch. Khim.* **1978**, *48*, 732.
(14) Lux, D.; Schwarz, W.; Hess, H.; Zeiss, W. *Z. Naturforsch., B* **1980**, *35B*, 269.

0020-1669/81/1320-1222$01.25/0

The extent of their dimerization depends primarily on the electronegativity of the phosphorus neighbor in the five-membered ring. When the ring atom attached to phosphorus is carbon, only monomers form,[15,16] with nitrogen, both monomers and dimers result,[17] and with oxygen, only dimers are known.[18-20]

In solution, diazadiphosphetidines, like monomeric phosphoranes, exhibit fluxional behavior. Their temperature-dependent NMR spectra imply a nondissociative ligand-exchange mechanism based on a square-pyramidal transition state, i.e., the Berry pseudorotation process.[21] For diazadiphosphetidines, concerted ligand exchange at the two phosphorus centers is required.[22,23] The exchange pathway is dependent on the relative apicophilicities of the ligands; the more electronegative ligands prefer apical positions of a trigonal bipyramid[24] or basal positions of a square pyramid.[25-28] In cyclic phosphoranes containing four- and five-membered rings, a competition for ligand placement arises between preferences based on electronegativity requirements and those based on ring strain[29] and the exchange process is expected to follow a more constrained pathway. For proper description of the exchange mechanism, the ground-state geometries should be obtained. They have been sufficiently characterized for diazadiphosphetidines having acyclic substituents (see above) but not for polycyclic derivatives.

Concerning the structure of the above-mentioned tricyclic systems, three possibilities arise which have the five-membered rings fused to the central diazadiphosphetidine ring (if we confine our attention to a trigonal-bipyramidal geometry for phosphorus and exclude diequatorial ring placement): the meridional II, the facial-cis (or -gauche) IV, and the facial-trans placement III of the fused rings.[2b] In solution they may interconvert by the sequence III ⇄ II ⇄ IV by concerted pseudorotational processes with an exocyclic substituent acting as a pivotal ligand.

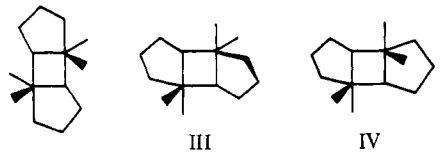

II III IV

Two principal factors seem important for the choice between these structural alternatives: (1) The desire for nitrogen to be planar, which is found for all diazadiphosphetidines I, will only be maintained in the meridional form II. (2) The presence of exocyclic phosphorus substituents more apicophilic than the atom attached to phosphorus in the five-membered ring promotes facial placement III or IV. X-ray crystal structures have been determined for two compounds of this type. However, in the first case[30] **1**, the two factors reinforce each other in suggesting the meridional conformation II, in agreement with the X-ray analysis. In the second example[2b] **2**, insufficient competition of factors is present as the exocyclic and endocyclic ligands at phosphorus have similar apicophilicities. Again the structural form is of the type II.

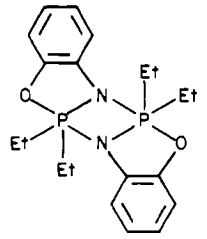

1

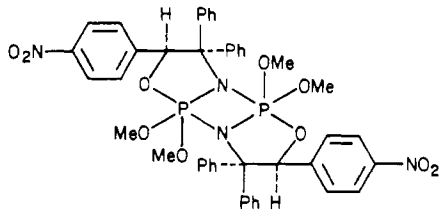

2

To ascertain the relative importance of the factors involved, we undertook the NMR study of tetrafluoro- and tetrachloro-substituted dimers of 1,3,4,2-oxadiaza- and 1,2,4,3-triazaphospholes **3** and **4**, respectively, as well as the X-ray crystallographic analysis of both members **4a** and **4b**. Since spirocyclic phosphoranes have been shown to form a series of structures extending from the trigonal bipyramid to the rectangular pyramid,[25,31] consideration of this factor as a competing structural influence is also examined.

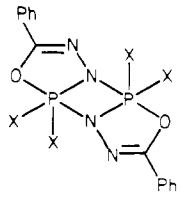

3a, X = F
b, X = Cl

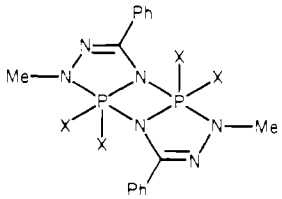

4a, X = F
b, X = Cl

Experimental Section

Preparation of 5,5,10,10-Tetrahalo-2,7-diphenyl[1,3,2,4]diazadiphospheto[2,1-*b*:4,3-*b'*]bis[1,3,4,2λ⁵]oxdiazaphospholes (3). The chloro derivative **3b** was obtained as described.[19,20] For the fluoro derivative **3a**, 10 mmol of **3b** and 15 mmol of SbF_3 were heated to reflux in 50 mL of benzene or carbon tetrachloride. The exchange was complete after 12 h. After removal of solvent, the residue was recrystallized from $CHCl_3$; mp 175–176 °C. Anal. Calcd for $C_{14}H_{10}F_4N_4O_2P_2$: C, 41.60; H, 2.49; N, 13.86. Found: C, 41.85; H, 3.00; N, 13.72.

Preparation of 5,5,10,10-Tetrahalo-1,6-dimethyl-3,8-diphenyl-[1,3,2,4]diazadiphospheto[2,1-*c*:4,3-*c'*]bis[1,2,4,3λ⁵]triazaphospholes (4). The chloro derivative **4b** was obtained as described,[17] and the fluoro derivative **4a**, by the above procedure from **4b**. There is considerable loss of product during recrystallization; mp 183–185 °C. Anal. Calcd for $C_{16}H_{16}F_4N_6P_2$: C, 44.64; H, 3.75; N, 19.52; Found: C, 44.12; H, 4.22; N, 19.27.

Crystallographic Study of 4a and 4b

Space Group Determination and Data Collection for $(PhMeCN_3PF_2)_2$ (4a). A nearly cubic crystal with an edge length

(15) Schmidpeter, A.; Zeiss, W. *Angew. Chem.* **1971**, *83*, 397; *Angew. Chem., Int. Ed. Engl.* **1971**, *10*, 396.
(16) Sheldrick, W. S.; Schomburg, D.; Schmidpeter, A.; von Criegern, Th. *Chem. Ber.* **1980**, *113*, 55.
(17) Schmidpeter, A.; Luber, J.; Tautz, H. *Angew. Chem.* **1977**, *89*, 554; *Angew. Chem., Int. Ed. Engl.* **1977**, *16*, 546.
(18) Schmidpeter, A.; Luber, J. *Phosphorus* **1974**, *5*, 55.
(19) Schmidpeter, A.; Luber, J. *Chem. Ber.* **1975**, *108*, 820.
(20) Schmidpeter, A.; Luber, J.; von Criegern, Th. *Z. Naturforsch., B* **1977**, *32B*, 845.
(21) Berry, R. S. *J. Chem. Phys.* **1960**, *32*, 933.
(22) Harris, R. K.; Woplin, J. R.; Dunmur, R. E.; Murray, M.; Schmutzler, R. *Ber. Bunsenges. Phys. Chem.* **1972**, *76*, 44.
(23) Schlak, O.; Schmutzler, R.; Harris, R. K.; Murray, M. *J. Chem. Soc., Chem. Commun.* **1973**, 23.
(24) Muetterties, E. L.; Mahler, W.; Schmutzler, R. *Inorg. Chem.* **1963**, *2*, 613.
(25) Holmes, R. R.; Deiters, J. A. *J. Am. Chem. Soc.* **1977**, *99*, 3318.
(26) Muetterties, E. L.; Schunn, R. A. *Q. Rev., Chem. Soc.* **1966**, *20*, 245.
(27) Rauk, A.; Allen, L. C.; Mislow, K. *J. Am. Chem. Soc.* **1972**, *94*, 3035.
(28) Strich, A.; Veillard, A. *J. Am. Chem. Soc.* **1973**, *95*, 5574.
(29) (a) Westheimer, F. H. *Acc. Chem. Res.* **1968**, *1*, 70. (b) Ramirez, F. *Ibid.* **1968**, *1*, 168. (c) Muetterties, E. L. *Ibid.* **1970**, *3*, 266.
(30) Kabachnik, M. I.; Gilyarov, V. A.; Tikhonina, N. A.; Kalinin, A. E.; Andrianov, V. G.; Struchkov, Yu. T.; Timofeeva, G. I. *Phosphorus*, **1974**, *5*, 65.
(31) Holmes, R. R. *Acc. Chem. Res.* **1979**, *12*, 257.

Table I. Chemical Shifts δ[a] and Coupling Constants J [Hz]

	3a[b]	3b	4a	4b	5	6
$\delta(^{31}P)$	−51	−52.2[20]	−61.5	−63[17]	−53.6	
$\delta(^{19}F)$	−70.4		−57.5		−67.1	−52.9
$^2J_{PP}$	+277.7		+154			
$^1J_{PF}$	−992.6		−947		−910	−906
$^3J_{PF}$	+27.6		+31.5			
$^2J_{FF}$	−28.9					
$^4J_{FF}$	+8.1 (trans) −0.7 (gauche)		+4.9 (av)			
$\delta(^1H(CH_3))$			3.05	3.43		
$\lvert^3J_{PH} + {}^5J_{PH}\rvert$			8.2	16.4		
$\lvert^4J_{FH} + {}^6J_{FF}\rvert$			1			
$\delta(^{13}C(CH_3))$			37.6	39.9		
$\lvert^2J_{PC} + {}^4J_{PC}\rvert$			10.9	9.5		
$\delta(^{13}C(C\text{-}5))$			146.8	146.6		
$\lvert^2J_{PC} + {}^4J_{PC}\rvert$			18.6	18.9		

[a] Relative to H_3PO_4, $CFCl_3$, and Me_4Si, respectively; negative values indicate a high-field shift. [b] J for 3a are taken from the analysis by DAVINS.[29]

of approximately 0.3 mm was cut from a larger crystal and mounted inside of a thin-walled glass capillary tube, which was sealed as a precaution against moisture sensitivity. Preliminary investigations using an Enraf-Nonius CAD 4 automated diffractometer and graphite-monochromated molybdenum radiation (fine-focus tube, 45 kV, 20 mA, takeoff angle 3.1°, $\lambda(K\alpha_1)$ 0.709 30 Å, $\lambda(K\alpha_2)$ 0.713 59 Å) showed monoclinic ($2/m$) symmetry. From the observed extinctions $0k0$, $k = 2n + 1$, and $h0l$, $h + l = 2n + 1$, the space group was uniquely determined as $P2_1/n$ (alternate setting of $P2_1/c$-C_{2h}^5).[32] The lattice constants as determined by the least-squares refinement of the diffraction geometry for 25 reflections having $10.66° \le \theta_{Mo K\bar{\alpha}} \le 14.82°$ and measured at an ambient laboratory temperature of 22 ± 2 °C are a = 11.344 (7) Å, b = 11.617 (5) Å, c = 14.254 (11) Å, and β = 96.83 (6)°. A unit cell content of 4 molecules gives a calculated volume of 16.7 Å^3 per nonhydrogen atom, which falls in the range expected for such molecules. The assignment of $Z = 4$ was confirmed by successful solution and refinement of the structure.

Data were collected with use of the θ–2θ scan mode with a θ scan range of $(0.65 \pm 0.35 \tan\theta)°$ centered about the calculated Mo K$\bar{\alpha}$ peak position. The scan range was actually extended an extra 25% on either side of the aforementioned limits for the measurement of background radiation. The scan rates varied from 0.69 to 4.0°/min, the rate to be used for each reflection having been determined by a prescan. The intensity, I, for each reflection is then given by $I = [(FF)/S][P - 2(B_1 + B_2)]$ where P are the counts accumulated during the peak scan, B_1 and B_2 are the left and right background counts, S is an integer which is inversely proportional to the scan rate, and FF is either unity or a multiplier to account for the occasional attenuation of the diffracted beam. The standard deviations in the intensities, σ_I, were computed as $\sigma_I^2 = [(FF)^2/S^2][P + 4(B_1 + B_2)] + 0.002I^2$. A total of 3271 independent reflections ($+h,+k,\pm l$) having $2° \le 2\theta_{Mo K\bar{\alpha}} \le 50°$ was measured. Six standard reflections, monitored after every 12 000 s of X-ray exposure time, gave no indication of crystal deterioration or loss of alignment. No corrections were made for absorption ($\mu_{Mo K\bar{\alpha}}$ = 0.295 mm^{-1}), and the intensities were reduced to relative amplitudes by means of standard Lorentz and polarization corrections, including corrections for the monochromator.

Solution and Refinement for 4a. Initial coordinates for 27 of the 28 independent nonhydrogen atoms were obtained by direct methods (MULTAN), while initial coordinates for the remaining independent nonhydrogen atom were obtained by standard Fourier difference techniques. Isotropic unit-weighted full-matrix least-squares refinement[33] of the structural parameters for these 28 atoms and a scale factor gave a conventional residual $R = \sum||F_o| - |F_c||/\sum|F_o|$ of 0.083 and a weighted residual $R_w = [\sum w(|F_o| - |F_c|)^2/\sum w|F_o|^2]^{1/2}$ of 0.087 for the 1517 reflections having $I \ge 3\sigma_I$ and $(\sin\theta)/\lambda \le 0.52$ Å^{-1}. Anisotropic refinement then gave R = 0.059 and R_w = 0.068 for the 1618 reflections having $I \ge 2\sigma_I$. Initial coordinates for the independent methyl hydrogen atoms were then obtained from a Fourier difference synthesis, while initial coordinates for the 10 independent aromatic hydrogen atoms were inferred from the required geometry of the molecule. Subsequent refinement including these 16 hydrogen atoms as isotropic scatterers and using variable weights ($w^{1/2} = 2LpF_o/\sigma_I$) gave R = 0.035 and R_w = 0.046 for 1618 reflections. The final cycles of refinement included the high-angle data and led to R = 0.042, R_w = 0.051, and GOF[34] = 1.39 for the 2059 reflections having $I \ge 2\sigma_I$ and $2° \le 2\theta_{Mo K\bar{\alpha}} \le 50°$. During the last cycle of refinement the largest shift in any parameter was 0.1 times its estimated standard deviation (esd). A final Fourier difference synthesis showed a maximum density of 0.24 e/Å^3.

Space Group Determination and Data Collection for $(PhMeCN_3PCl_2)_2$ (4b). Experimental conditions were the same as those described for **4a**. Crystals of **4b** are extremely moisture sensitive. An approximately cube-shaped crystal having fresh faces and an edge length of about 0.38 mm was cut from a larger crystal and quickly sealed inside a thin-walled glass capillary tube. Preliminary diffractometric investigations showed monoclinic ($2/m$) symmetry and the extinctions $0k0$, $k = 2n + 1$, and $h0l$, $l = 2n + 1$, consonant with the uniquely determined space group $P2_1/c$.[32] The lattice constants based on 25 reflections having $10.01° \le \theta_{Mo K\bar{\alpha}} \le 14.76°$ are a = 6.585 (2) Å, b = 21.383 (9) Å, c = 15.824 (7) Å, and β = 103.89 (4)°, giving a unit cell volume consistent with $Z = 4$. A total of 3790 independent reflections was measured, monitoring six standard reflections. No corrections were made for absorption ($\mu_{Mo K\bar{\alpha}}$ = 0.709 mm^{-1}).

Solution and Refinement for 4b. Conditions for solution and refinement of **4b** were the same as described for **4a** unless otherwise noted. Initial coordinates for 16 of the 28 independent nonhydrogen atoms were obtained by direct methods, while initial coordinates for the remaining 12 independent nonhydrogen atoms were obtained by standard Fourier difference techniques. Isotropic unit-weighted refinement of the structural parameters for these 28 atoms and a scale factor gave R = 0.094 and R_w = 0.096, with subsequent anisotropic refinement leading to R = 0.051 and R_w = 0.059 for the 2078 reflections having $I \ge 2\sigma_I$ and $(\sin\theta)/\lambda \le 0.52$ Å^{-1}. Coordinates for the 6 independent methyl hydrogen atoms were then taken from a Fourier difference synthesis while initial coordinates for the 10 aromatic hydrogen atoms were inferred from the required geometry of the molecule. Refinement using variable weights and including these 16 hydrogen atoms as isotropic scatterers (fixed parameters for the 6 methyl hydrogen atoms) led to R = 0.032 and R_w = 0.044. Inclusion of the high-angle data in the refinement then led to the final values of R = 0.036, R_w = 0.046, and GOF = 1.34[34] for the 2855 reflections having $I \ge 2\sigma_I$ and $2° \ge 2\theta_{Mo K\bar{\alpha}} \le 50°$. During the final cycle of refinement the largest shift in any parameter was 0.02 times its esd. A final Fourier difference synthesis showed a maximum density of 0.38 e/Å^3.

Computations were done on a CDC Cyber-175 computer using LINEX (a modification of the Busing and Levy full-matrix least-squares

(32) "International Tables for X-ray Crystallography"; Kynoch Press: Birmingham, England, 1969; Vol. I, p 99.

(33) The function minimized was $\sum w(|F_o| - |F_c|)^2$. Mean atomic scattering factors were taken from: Reference 32, 1974; Vol. IV, pp 72–98. Real and imaginary dispersion corrections for P and F were taken from the same source, pp 149–150.

(34) GOF = $[\sum w(|F_o| - |F_c|)^2/(N_o - N_v)]^{1/2}$ where for **4a** N_o = number of observations = 2059 and N_v = number of variables = 317 and for **4b** N_o = 2855 and N_v = 293.

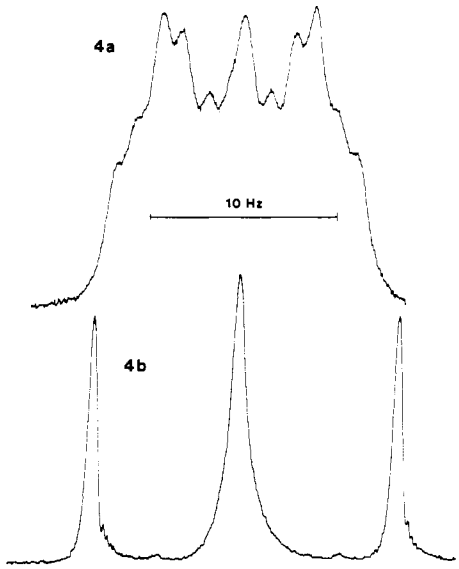

Figure 1. Methyl proton NMR signal of **4a** and **4b**.

program, ORFLS), Johnson's thermal ellipsoid plot program (ORTEP), the Oak Ridge Fortran function and error program (ORFFE), Zalkin's Fourier program (FORDAP), and several locally written programs.

Results and Discussion

Preparative Aspects. The chloro-substituted tricyclodiphosphoranes **3b**[19,20] and **4b**[17] are formed in a cyclocondensation by reaction of phosphorus pentachloride with benzohydrazide and 1-methylbenzamidrazone hydrochloride, respectively. Chloride/fluoride exchange to give **3a** and **4a** is achieved with antimony trifluoride.

3a and **4a** are sensitive to moisture. Trace hydrolysis in solution is readily detected by additional signals in the ^{19}F and ^{31}P NMR spectra (Table I) indicating the monomeric trifluorophosphoranes **5** and **6**, respectively. Addition of triethylamine reconverts them to **3a** and **4a**.

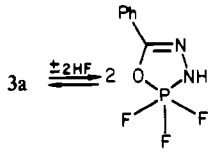

5

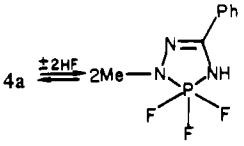

6

NMR Spectra. The dimeric and symmetric structures of **3** and **4** are readily apparent from their NMR spectra. Thus the ^{31}P shifts (Table I) are typical of σ^5P. The methyl proton signal of **4b** (Figure 1) is a pseudotriplet as expected[35] for the X part of an $[AX_3]_2$ spin system in case of $|J_{AA}| \gg L_{AX}$, i.e., for phosphorus–phosphorus coupling which is strong compared to the difference of the two phosphorus–proton couplings $L_{AX} = J_{AX} - J'_{AX}$. In **4a** the signal (Figure 1) is further split by coupling with the two magnetically nonequivalent pairs of fluorine. The $^{19}F\{^1H\}$ and $^{31}P\{^1H\}$ NMR spectra of **3a** and **4a** represent the X and A regions, respectively, of a $[A[X]_2]_2$ spin system[22] (Figures 2–5). Three of the six coupling constants for this system, $^2J_{PP}$, $^1J_{PF}$, and $^3J_{PF}$, are readily obtained from the spectra as well as N_{XX}, which is the sum of the two different long-range phosphorus–fluorine coupling constants $^4J_{FF}$. However, due to insufficient resolution L_{XX}, their difference, is not obtained. The spectra are predicted[22] to be insensitive to the value of the geminal fluorine–fluorine coupling $^2J_{FF}$.

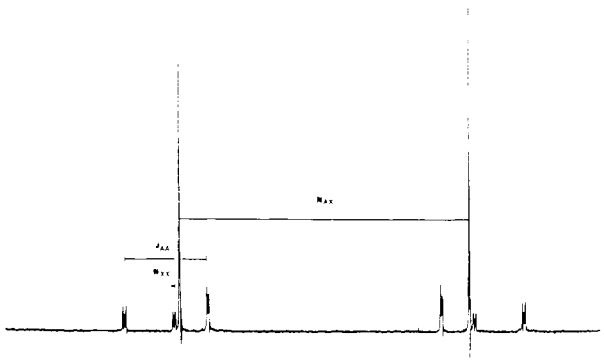

Figure 2. $^{19}F\{^1H\}$ spectrum of **3a**.

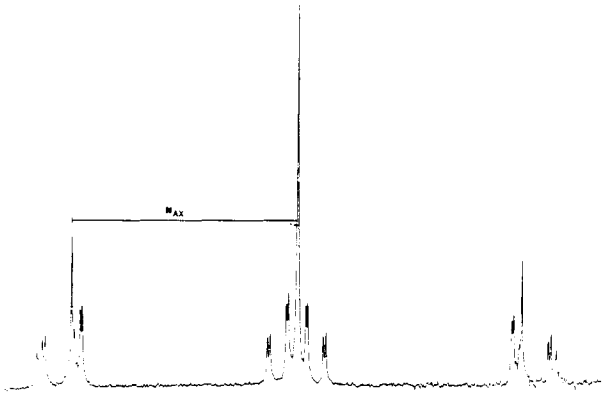

Figure 3. $^{31}P\{^1H\}$ spectrum of **3a**.

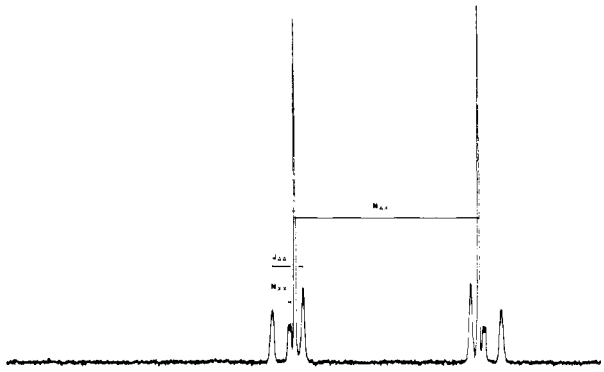

Figure 4. $^{19}F\{^1H\}$ spectrum of **4a**.

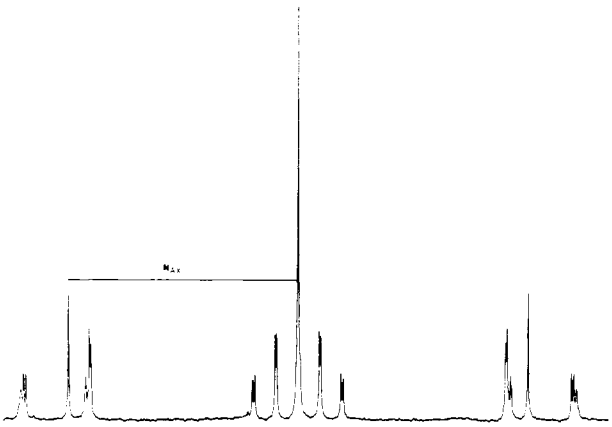

Figure 5. $^{31}P\{^1H\}$ spectrum of **4a**.

(35) Harris, R. K. *Can. J. Chem.* **1964**, *42*, 2275.

Table II. Atomic Coordinates in Crystalline $(PhMeCH_3PF_2)_2$ (4a)[a]

atom type[b]	10^4x	10^4y	10^4z
P	2652 (1)	3874 (1)	8416 (1)
P′	4292 (1)	2324 (1)	8933 (1)
F1	1320 (2)	4017 (2)	8624 (2)
F2	2304 (2)	3850 (2)	7324 (1)
F1′	5698 (2)	2406 (2)	9183 (1)
F2′	4378 (2)	1422 (2)	8139 (1)
N1	4180 (2)	3632 (2)	8414 (2)
N3	4196 (2)	5536 (3)	8761 (2)
N4	3012 (2)	5175 (3)	8802 (2)
N1′	2750 (2)	2493 (2)	8794 (2)
N3′	2980 (2)	1427 (3)	10120 (2)
N4′	4145 (2)	1713 (3)	9955 (2)
C2	4826 (3)	4654 (3)	8569 (2)
CM	2252 (4)	6112 (4)	9103 (4)
CA1	6088 (3)	4773 (3)	8444 (2)
CA2	6623 (3)	3998 (4)	7880 (3)
CA3	7799 (4)	4139 (4)	7734 (3)
CA4	8439 (4)	5052 (4)	8153 (3)
CA5	7927 (4)	5806 (4)	8715 (3)
CA6	6747 (3)	5676 (4)	8862 (3)
C2′	2226 (3)	1882 (3)	9484 (2)
CM′	5059 (4)	1352 (4)	10720 (2)
CB1	936 (3)	1714 (3)	9484 (2)
CB2	166 (3)	1707 (3)	8654 (3)
CB3	−1033 (4)	1501 (4)	8687 (3)
CB4	−1461 (4)	1305 (3)	9532 (4)
CB5	−704 (4)	1307 (4)	10358 (3)
CB6	500 (3)	1509 (3)	10337 (3)

[a] Numbers in parentheses are estimated standard deviations in the last significant figure. [b] Atoms are labeled to agree with Figure 6.

Table III. Atomic Coordinates in Crystalline $(PhMeCN_3PCl_2)_2$ (4b)[a]

atom type	10^4x	10^4y	10^4z
P	3752 (1)	1556.8 (3)	4382.8 (5)
P′	3787 (1)	2093.1 (4)	2880.6 (5)
Cl1	3290 (1)	625.0 (4)	4695.8 (5)
Cl2	1611 (1)	1914.8 (4)	4985.8 (6)
Cl1′	5771 (1)	2772.6 (4)	2560.1 (6)
Cl2′	1090 (1)	2548.6 (4)	2300.5 (6)
N1	4446 (3)	2266 (1)	3948 (1)
N3	7011 (4)	2191 (1)	5166 (2)
N4	6156 (4)	1585 (1)	5048 (2)
N1′	2623 (3)	1462 (1)	3315 (1)
N3′	3086 (4)	1023 (1)	2089 (2)
N4′	4376 (4)	1559 (1)	2202 (2)
C2	6113 (4)	2552 (1)	4539 (2)
CM	7164 (6)	1170 (2)	5769 (3)
CA1	6610 (4)	3223 (1)	4557 (2)
CA2	5119 (5)	3662 (1)	4197 (2)
CA3	5567 (6)	4294 (2)	4299 (2)
CA4	7506 (7)	4485 (2)	4765 (3)
CA5	9008 (6)	4048 (2)	5135 (3)
CA6	8581 (5)	3423 (2)	5025 (2)
C2′	2192 (5)	962 (1)	2728 (2)
CM′	5387 (7)	1634 (2)	1474 (2)
CB1	707 (5)	460 (1)	2754 (2)
CB2	−2343 (6)	53 (2)	3144 (3)
CB3	−963 (5)	543 (2)	3139 (2)
CB4	−2073 (7)	−513 (2)	2783 (3)
CB5	946 (6)	−114 (2)	2374 (2)
CB6	−446 (7)	−596 (2)	2389 (3)

[a] Footnotes to Table II apply, except that atoms are labeled to agree with Figure 7.

In fact, the synthesized spectra did not respond significantly to a variation of the $^2J_{FF}$ value in the range ±300 Hz. Using automated analysis of the ^{19}F and ^{31}P spectrum of **3a** with the aid of the computer program DAVINS,[36] we obtained a best solution (R = 1.72) which gave $^2J_{FF}$ equal to −28.9 Hz (with a standard deviation of 0.8 Hz). In unsymmetric diazadiphosphetidines, the axial–equatorial geminal fluorine–fluorine coupling has been found to be around −50 Hz.[37]

From the observed equivalence of the two fluorine ligands for **3a** and **4a**, structure II is indicated. However, the NMR data are also in agreement with ground-state structures of the type III or IV if rapid intramolecular ligand exchange is taking place. Equatorial fluorine atoms generally give rise to a higher field ^{19}F chemical shift and a larger $|^1J_{PF}|$ coupling constant than do apical fluorines in the same system, but when $^1J_{PF}$ values are compared in different phosphoranes, this dependency may be obscured by other factors.[37] The relatively high values obtained for **3a** and **4a** (Table I) would lead one to suspect a type II structure with both fluorines equatorial, albeit no straightforward conclusion is possible.

$^2J_{PP}$ in diazadiphosphetidines generally increases with the substituent electronegativity.[22,37] Accordingly, it is much higher for **3a** than for **4a**. An even more pronounced increase is effected by the presence of the fused ring system. This may account for the very high value of $^2J_{PP}$ for **3a**, which is above the value of 210 Hz[38] observed for $(F_3PNMe)_2$. In fact, this is the highest phosphorus–phosphorus coupling yet observed in diazadiphosphetidines.

Molecular Structures of 4a and 4b. The atom-labeling schemes for **4a** and **4b** are shown in the ORTEP plots in Figures 6 and 7, respectively. Atomic coordinates appear in Tables II and III. Pertinent bond lengths and angles are given in Table IV. Thermal parameters and bond parameters for

Table IV. Bond Lengths and Angles Involving the Fused Ring Systems and Phosphorus Atoms for $(PhMeCN_3PX_2)_2$, X = F (4a) and X = Cl (4b)[a]

	X = F		X = Cl	
	unprimed	primed	unprimed	primed
	Bond Lengths, Å			
P-X1	1.583 (2)	1.594 (2)	2.093 (1)	2.096 (1)
P-X2	1.559 (3)	1.554 (2)	2.032 (1)	2.041 (1)
P-N1	1.756 (3)	1.749 (3)	1.770 (2)	1.770 (2)
P-N4	1.643 (3)	1.647 (3)	1.679 (3)	1.675 (3)
P-N1′	1.692 (3)	1.688 (3)	1.686 (3)	1.681 (2)
N1-C2	1.398 (4)	1.401 (4)	1.400 (4)	1.401 (4)
C2-N3	1.297 (4)	1.283 (4)	1.283 (4)	1.293 (4)
N3-N4	1.416 (4)	1.409 (4)	1.409 (3)	1.412 (3)
N4-CM	1.482 (5)	1.473 (5)	1.471 (4)	1.472 (4)
C2-CPh	1.471 (5)	1.477 (5)	1.470 (4)	1.459 (4)
	Bond Angles, Deg			
X1-P-X2	93.1 (1)	93.2 (1)	95.2 (1)	94.9 (1)
X1-P-N1	168.9 (1)	168.3 (1)	166.7 (1)	167.3 (1)
X1-P-N4	92.6 (1)	91.8 (1)	93.1 (1)	93.7 (1)
X1-P-N1′	93.9 (1)	93.8 (1)	94.0 (1)	93.7 (1)
X2-P-N1	97.4 (1)	98.1 (1)	97.6 (1)	97.3 (1)
X2-P-N4	112.0 (1)	112.0 (2)	110.4 (1)	110.3 (1)
X2-P-N1′	107.4 (1)	107.2 (1)	109.1 (1)	109.5 (1)
N1-P-N4	86.7 (1)	86.7 (1)	85.4 (1)	85.3 (1)
N1-P-N1′	79.7 (1)	80.0 (1)	78.8 (1)	79.0 (1)
N4-P-N1′	139.6 (1)	140.0 (2)	139.0 (1)	138.6 (1)
P-N1-P′	99.6 (1)	99.7 (1)	100.0 (1)	99.8 (1)
P-N1-C2	111.2 (2)	111.4 (2)	110.5 (2)	111.2 (2)
C2-N1-P′	133.1 (2)	133.4 (2)	137.6 (2)	136.5 (2)
P-N4-CM	130.0 (3)	129.8 (3)	130.3 (2)	130.2 (2)
P-N4-N3	117.2 (2)	116.4 (2)	113.7 (2)	114.2 (2)
CM-N4-N3	112.5 (3)	113.6 (3)	111.2 (2)	111.1 (3)
N4-N3-C2	108.9 (3)	110.1 (3)	110.8 (2)	110.9 (2)
N1-C2-N3	114.4 (3)	113.7 (3)	113.3 (2)	112.5 (3)
N1-C2-CPh	124.1 (3)	124.7 (3)	125.1 (2)	125.0 (3)
N3-C2-CPh	121.3 (3)	121.5 (3)	120.8 (3)	122.0 (3)

[a] Atoms are labeled to agree with Figures 6 and 7. Primed atoms are related to unprimed ones by the pseudo-twofold axis, where P-N1′ goes into P′-N1 etc.

(36) Stephenson, D. S.; Binsch, G. *J. Magn. Reson.* **1980**, *73*, 395, 409.
(37) Harris, R. K.; Wazeer, M. I. M.; Schlak, O.; Schmutzler, R. *J. Chem. Soc., Dalton Trans.* **1974**, 1912.
(38) Harris, R. K.; Woodman, C. M. *Mol. Phys.* **1966**, *10*, 437.

Table V. Deviations (Å) from Some Least-Squares Mean Planes for $(PhMeCN_3PF_2)_2$ (4a)[a,b]

	I	II	III	IV	V	VI	VIIA	VII	VIII	
P	0.069	−0.016	−0.069	(−0.228)	−0.013	0.0	0.053	0.0	CA1	−0.004
F1		0.044	(0.125)		(0.048)				CA2	0.003
F2	−0.034	−0.060							CA3	0.001
N1′	−0.017						−0.053	0.0	CA4	−0.005
N4	−0.019		0.078	0.008	0.039	(0.052)	(1.126)	(1.014)	CA5	0.004
N1		0.032	0.054	−0.008			−0.056	0.0	CA6	0.000
C2			−0.018	0.014				(0.622)		
N3			−0.045	−0.014	−0.012	0.0				
CM			(0.180)		−0.013	0.0				
P′			(1.157)				0.056	(0.216)		
N4′							(1.130)			

	I′	II′	III′	IV′	V′	VI′	VII′	VIII′	
P′	0.062	0.028	−0.074	(−0.230)	−0.007	0.0	0.0	CB1	0.003
F1′		−0.013	(0.137)		(0.033)			CB2	−0.001
F2′	−0.025	−0.003						CB3	−0.001
N1	−0.024						0.0	CB4	0.001
N4′	−0.014		0.081	0.005	0.020	(0.026)	(1.011)	CB5	0.001
N1′		−0.012	0.051	−0.006			0.0	CB6	−0.003
C2′			−0.024	0.010			(0.609)		
N3′			−0.034	−0.010	−0.006	0.0			
CM′			(0.254)		−0.007	0.0			
P			(1.145)				(0.217)		

[a] Deviations in parentheses are for atoms not included in the calculation of the plane. [b] Selected dihedral angles between planes indicated: I and II, 87.0°; I′ and II′, 87.6°; III and VIIA, 37.0°; III′ and VIIA, 36.7°; III and III′, 73.8°; III and VIII, 22.3°; III′ and VIII′, 26.4; VII and VII′, 9.5°; III and VII, 33.5°; III′ and VII′, 33.0.

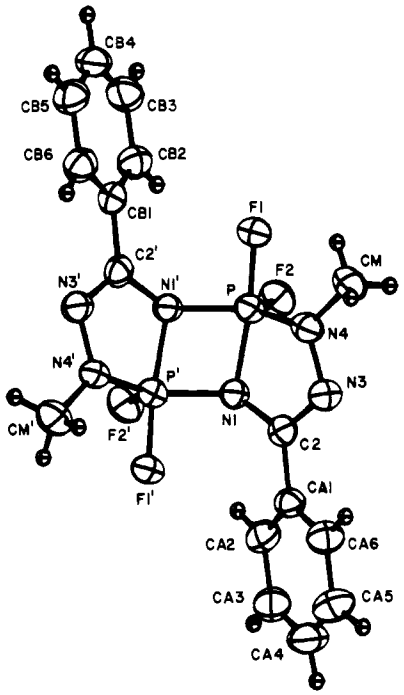

Figure 6. ORTEP plot of $(PhMeCN_3PF_2)_2$ (**4a**) with thermal ellipsoids at the 50% probability level for nonhydrogen atoms. Hydrogen atoms are represented by spheres of arbitrary radius.

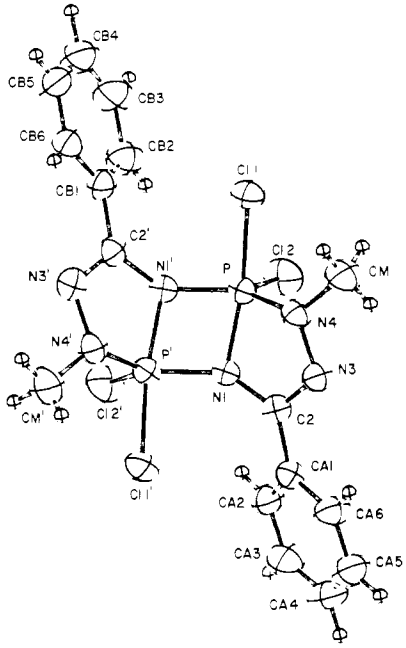

Figure 7. ORTEP plot of $(PhMeCN_3PCl_2)_2$ (**4b**) with thermal ellipsoids at the 50% probability level for nonhydrogen atoms. Hydrogen atoms are represented by spheres of arbitrary radius.

phenyl groups and those involving hydrogen atoms are listed as supplementary material at the end of this article.

As seen in Figures 6 and 7, the basic structural type is the same for **4a** and **4b**, i.e., the cis-facial ring arrangement IV. Both have a pseudo-twofold axis relating the halves of the dimer. Primed atoms go into unprimed ones by this pseudo-twofold axis, and the A phenyl ring goes into the B phenyl ring. The high degree of structural similarity between the fluoro and chloro derivatives is evident on examining the corresponding angles at the phosphorus centers illustrated in Figure 8. The X1–P–N1 (X1′–P′–N1′) and N4–P–N1′ (N4′–P′–N1) angles are centered around 168 and 139°, respectively, for both derivatives. Relative to the ideal trigonal bipyramid, the senses of the angles are such that as the axial angles close, the equatorial angles open. This indicates that the structural distortion is following a C_{2v} constraint. This is further emphasized by the nearness of the atoms to the equatorial axial least-squares mean planes I (I′) and II (II′) in Tables V and VI for each derivative. Relative bond lengths are as expected, $P–N_{ax} > P–N_{eq}$ and $P–X_{ax} > P–X_{eq}$.

With use of the dihedral angle method as applied to cyclic phosphoranes,[25,31,39] the geometry at the phosphorus atoms is displaced 52% for **4a** and 53% for **4b** from the trigonal bipyramid toward the square pyramid (based on unit bond

(39) Holmes, R. R. *ACS Monogr.* **1980**, *No. 175.*

Table VI. Deviations (Å) from Some Least-Squares Mean Planes for $(PhMeCN_3PCl_2)_2$ (4b)[a,b]

	I	II	III	IV	V	VI	VII	VIII
P	0.089	0.034	0.129	(0.468)	0.036	0.0	0.0	CA1 0.002
Cl1		−0.014	(−0.023)		(0.011)			CA2 0.003
Cl2	−0.011	−0.003						CA3 −0.003
N1′	−0.051						0.0	CA4 −0.002
N4	−0.027		−0.129	−0.011	−0.143	(−0.192)	(−1.031)	CA5 0.007
N1		−0.017	−0.151	0.011			0.0	CA6 −0.007
C2			0.040	−0.022			(−0.402)	
N3			0.110	0.022	0.045	0.0		
CM			(−0.038)		0.063	0.0		
P′			(−1.291)				(−0.348)	

	I′	II′	III′	IV′	V′	VI′	VII′	VIII′
P′	−0.090	−0.036	−0.124	(−0.452)	−0.035	0.0	0.0	CB1 0.006
Cl1′		0.015	(0.018)		(−0.016)			CB2 −0.001
Cl2′	0.012	0.003						CB3 −0.007
N1	0.051						0.0	CB4 0.010
N4′	0.027		0.125	0.012	0.139	(0.185)	(1.039)	CB5 −0.005
N1′		0.018	0.146	−0.011			0.0	CB6 −0.003
C2′			−0.038	0.021			(0.442)	
N3′			−0.107	−0.022	−0.043	0.0		
CM′			(0.038)		−0.061	0.0		
P			(1.303)				(0.349)	

[a] Deviations in parentheses are for atoms not included in the calculation of the plane. [b] Selected dihedral angles between planes indicated: I and II, 88.6°; I′ and II′, 89.0°; III and III′, 76.0°; III and VIII, 26.0°; III′ and VIII′, 24.3°; VII and VII′, 15.2°; III and VII, 31.1°; III′ and VII′, 31.7°.

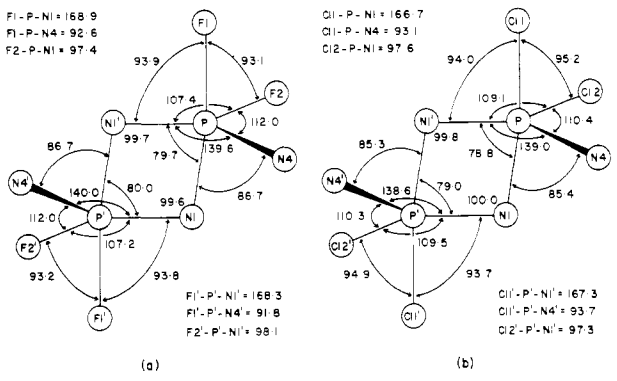

Figure 8. Selected bond angles for the diphosphorus moiety of $(PhMeCN_3PX_2)_2$: (a) **4a**, X = F; (b) **4b**, X = Cl.

vectors). The fit to the Berry coordinate (i.e., the C_{2v} constraint) is exact. This distortion places **4a** and **4b** one-fourth of the way along the coordinate connecting structure II and suggests this as a low-energy pseudorotation pathway IV ⇄ II. The latter may account for the appearance of equivalent fluorine atoms in the room-temperature NMR spectrum of **4a**. The extent of structural displacement toward II from IV may be viewed as a compromise between competing factors (discussed below) favoring these two structural types.

The two phosphorus centers (in each derivative) are connected via the nonplanar four-membered ring with P and P′ displaced in the same direction as N4, C2 and N4′, C2′, respectively; cf. planes VII and VII′ in Tables V and VI and their resultant dihedral angles. This folding is connected to the cis anellation IV of the five-membered rings as opposed to the trans anellation III. In the latter a molecular center of symmetry would replace the twofold axis to relate the halves of the dimer and would imply a planar diazadiphosphetidine ring. However, the angle sums at the nitrogen atoms N1 (N1′) could result in these atoms being pyramidal, as observed in the present case (see below). Thus, we can offer no data at present to adequately rationalize the appearance of IV instead of III. Examination of the intermolecular contacts gives little evidence that crystallographic packing is the cause.

In acyclic substituted and spirocyclic diazadiphosphetidines the angle sum at the nitrogen atoms are within 1 or 2° of 360°. In contrast, the N1 (N1′) nitrogen atoms have angle sums that average 344.2° for **4a** and 347.4° in **4b**. They are much closer to 360° for N4 (N4′): 359.8° in **4a** and 355.4° in **4b**; cf. deviations from the plane V (V′) of Tables V and VI. The greater N4 (N4′) planarity for the fluoro derivative coincides with a significantly smaller P–N4 (P′–N4′) bond length and indicates a stronger P–N π bond than in the chloro derivative.

Another feature worth noting is the planarity of the N4–N3–C2–N1 positions of the five-membered rings (planes IV and IV′ of Tables V and VI) as a result of the double bond at C2–N3. This ring rigidity coupled with the tendency for the ligand arrangement around N1 (N1′) to be planar may be causative in widening the N4–P–N1′ (N4′–P–N1) angles and displacing the structures **4a** and **4b** toward the square pyramid.[31]

Conclusion. The ground-state structures obtained for the tricyclic bridgehead phosphoranes **4a** and **4b** demonstrate the expected compromise between alternative II, which renders possible a planar arrangement around both nitrogen atoms adjacent to phosphorus, and IV, which places a halogen atom instead of nitrogen into the disposable apical site. The latter structural arrangement supports the strong tendency for an equatorial orientation of nitrogen atoms, presumably to maximize P–N π bonding.[40] The reduction in electronegativity provided by chlorine atoms in **4b** apparently is insufficient to cause any significant structural alteration. For compounds **3a** and **3b**, one might expect the structure to shift toward II owing to increased competition for apical occupancy brought on by the presence of electronegative ring oxygen atoms.

Acknowledgment. We are grateful to Dr. David S. Stephenson for the computer analysis, to Dr. Werner Zeiss for the synthesis of ^{19}F and ^{31}P NMR spectra, and also to Erwin Bacher for preparative help. The support of this research by the National Institutes of Health (Grant GM 21466), the National Science Foundation (Grant CHE 79-10036), and the Deutsche Forschungsgemeinschaft is gratefully acknowledged. We also thank the University of Massachusetts Computing Center for generous allocation of computer time.

(40) Hoffmann, R.; Howell, J. M.; Muetterties, E. L. *J. Am. Chem. Soc.* **1972**, *94*, 3047.

Registry No. **3a**, 76174-09-9; **3b**, 55498-97-0; **4a**, 76174-10-2; **4b**, 63148-50-5; SbF_3, 7783-56-4; **5**, 76174-11-3; **6**, 76174-12-4.

Supplementary Material Available: Compilations of observed and calculated structure factor amplitudes for **4a** and **4b**, thermal parameters (Table VII), refined hydrogen atom coordinates (Table VIII), and bond lengths and angles for phenyl groups and those involving hydrogen atoms (Table IX) for **4a**, and similar data for **4b** (Tables IX–XI) (24 pages). Ordering information is given on any current masthead page.

Contribution No. 6219 from the Department of Chemistry, California Institute of Technology, Pasadena, California 91125, and the School of Chemical Sciences, University of Illinois, Urbana, Illinois 61801

Binuclear Complexes of Macrocyclic Ligands: Variation of Magnetic Exchange Interaction in a Series of Six-Coordinate Iron(II), Cobalt(II), and Nickel(II) Complexes and the X-ray Structure of a Binuclear Iron(II) Macrocyclic Ligand Complex

CLIFFORD L. SPIRO,[1] SUSAN L. LAMBERT,[2] THOMAS J. SMITH,[1] EILEEN N. DUESLER,[2] ROBERT R. GAGNÉ,*[1] and DAVID N. HENDRICKSON*[2]

Received July 30, 1980

The X-ray crystal and molecular structure of $[LFe_2(Im)_4](BF_4)_2$, where Im is imidazole and L is the dianion of the binucleating ligand 11,23-dimethyl-3,7,15,19-tetraazatricyclo[19.3.1.1^{9,13}]hexacosa-2,7,9,11,13(26),14,19,21(25),22,24-decaene-25,26-diol, has been determined on a Syntex $P2_1$ diffractometer. A total of 2468 reflections at the $1.5\sigma(I)$ significance level were used to give final discrepancy indices of $R_1 = 0.082$ and $R_2 = 0.083$. The complex crystallizes in the monoclinic space group $C2/c$ in a cell having the dimensions $a = 21.060$ (5) Å, $b = 17.138$ (4) Å, $c = 12.172$ (2) Å, and $\beta = 108.82$ (2)°. The observed and calculated densities are 1.53 and 1.52 g/cm^3, respectively. Four formula units comprise the unit cell with half of the binuclear complex in the asymmetric unit. Discrete $[LF_2(Im)_4]^{2+}$ cations and BF_4^- anions were found. The binuclear cations are centrosymmetric with each iron(II) ion being six-coordinate by virtue of interactions with two nitrogen and two oxygen atoms of the binucleating ligand L and two nitrogen atoms each from the imidazole ligands. The ligand L is planar except for the two trimethylene bridges. The two iron ions are only 0.011 (1) Å out of this ligand plane with an Fe–Fe distance of 3.117 (2) Å and Fe–N(imidazole) distances of 2.218 Å. Variable-temperature (4.2–286 K) magnetic susceptibility data are given for the binuclear high-spin six-coordinate complexes $[LNi_2(py)_4](BF_4)_2$, $[LCo_2(py)_4](BF_4)_2$, $[LFe_2(py)_4](BF_4)_2$, $[LFe_2(Im)_4](BF_4)_2$, $[LFe_2(MeIm)_4](BF_4)_2$, and $[LFe_2(MeNic)_4](BF_4)_2$, where py is pyridine, Im is imidazole, MeIm is 1-methylimidazole, and MeNic is the methyl ester of isonicotinic acid. in each case an antiferromagnetic exchange interaction is present. The data were least-squares fit to the susceptibility equations resultant from the Hamiltonian $\hat{H} = -2J\hat{S}_1\cdot\hat{S}_2$ to give exchange parameters (J) of −23 (Ni^{2+}), −4.1 (Co^{2+}) and −7.5 cm^{-1} (Fe^{2+}) for the three pyridine complexes. Values of $J = -6.8$, −4.5, and −1.5 cm^{-1} were obtained for the other three high-spin iron(II) complexes with MeNic, MeIm, and Im axial ligands, respectively. It was found that there is little difference in the magnitude of magnetic exchange interaction between LM_2Cl_2 (M = Fe(II), Co(II), and Ni(II)) with five-coordinate metal ions and the corresponding complex in the $[LM_2(py)_4](BF_4)_2$ series with six-coordinate metal ions. An increase in antiferromagntic exchange interaction was expected for a six-coordinate complex compared to the analogous five-coordinate complex as a consequence of improved orbital overlap from the metal ion being in the plane of the binucleating ligand for the six-coordinate complex. This was not realized, possibly because the increased ligand field splitting in the six-coordinate complex attenuated the increased antiferromagnetic interaction.

Introduction

Complexes of the binucleating ligand LH_2 can be formed

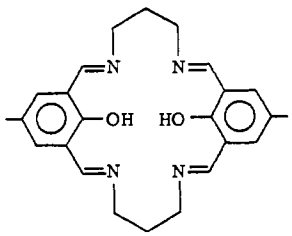

LH_2

from the condensation of 2 mol of 2,6-diformyl-4-methylphenol with 2 mol of 1,3-diaminopropane in the presence of divalent transition-metal ions.[3] X-ray structural work,[4,5] on $LCu_2Cl_2\cdot 6H_2O$ and $LCo_2Br_2\cdot CH_3OH$ has shown that the metal ion coordination geometry is square pyramidal with one halide ion bonded to each metal ion in an axial site. The cobalt(II) ion is further out of the L ligand plane (0.30 Å) than is the copper(II) ion (0.21 Å).

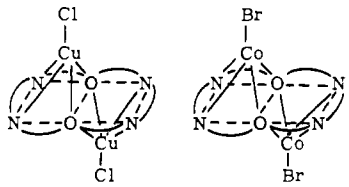

In a recent paper[6] we reported variable-temperature magnetic susceptibility data for a series of complexes of L including $LCu_2Cl_2\cdot 6H_2O$, $LNi_2Cl_2\cdot 2H_2O$, $LCo_2Br_2\cdot CH_3OH$, LMn_2Cl_2, and LFe_2Cl_2. The magnetic exchange interaction observed for each complex was assessed with the isotropic spin Ham-

(1) California Institute of Technology.
(2) University of Illinois.
(3) Pilkington, N. H.; Robson, R. *Aust. J. Chem.* **1970**, *23*, 2225.
(4) Hoskins, B. F.; Williams, G. A. *Aust. J. Chem.* **1975**, *28*, 2607.
(5) Hoskins, B. F.; McLeod, N. J.; Schaap, H. A. *Aust. J. Chem.* **1976**, *29*, 515.
(6) Lambert, S. L.; Hendrickson, D. N. *Inorg. Chem.* **1979**, *18*, 2683.

0020-1669/81/1320-1229$01.25/0